South Asian Journal of Engineering and Technology Research Article

Open Access Full Text Article 146(2024) 66- 78 DOI: 10.26524/sajet.2024.14.26

Studies on the growth and characterization of L-Asparagine Monohydrate Admixtured with Dl- Malic Acid Single Crystals

N. Rajasekar[a*], K. Balasubramanian[b]

[a]Research scholar

[a,b]PG & Research Department of physics, The M.D.T Hindu college, Tirunelveli - 627010, Tamil Nadu, India.

[a,b] (Affiliated to Manonmaniam sundaranar university, Abishekapatti, Tirunelveli, Tamilnadu, India)

Corresponding author.
Correspondence: N. Rajasekar
E-mail: **rs9012618@gmail.com**

Article info
Received 3th August 2024 Received in revised form 2 September 2024
Accepted 4 October 2024

Keywords
organic acid, Slow evapouration method, XRD, FTIR, UV, SEM, EDAX, and LDT

https://sajet.in/index.php/journal/article/view/296

Abstract

Single crystal of L-Asparagine monohydrate admixtured with DL- malic acid (LAMDLM) has been grown by slow evaporation solution growth technique by using deionized water as solvent at room temperature. Optically clear single crystals having dimensions up to 4mm x 3mm x 1mm. Powder X-ray diffraction analysis reveals that LAMDLM crystal crystallizes by Orthorhombic system with the space group of $P2_12_12_1$. The physical phase of the product was confirmed by powder x-ray diffraction analysis. The Fourier Transform Infrared (FTIR) spectra of all grown crystals have been recorded in the wavenumber range of 500-4500 cm^{-1} by KBr pellet technique and the associated functional groups of the grown crystals. The optical parameters, such as optical band gap energy, transparency (%) and absorbance were calculated parameters using UV-Vis Transmittance data in the spectral range of wavelength 190-1100 nm. The Multilayer plate-like pattern of growth was observed by Scanning electron microscopy. The presence of L-Asparagine malate was confirmed by EDAX analysis. Incorporation of Various elements present in L-Asparagine malate in the crystal was confirmed by Energy Dispersive X-ray Analysis (EDX). The laser damage threshold for the grown crystal was measured using Nd:YAG Laser. The laser damage threshold value was found to be 3.6 GW/cm^2.

1. Introduction

Nonlinear optics plays an important role in optical communication, Optical storage, optoelectronic technologies and photonics. Most of the amino acids are good Nlo properties. Organic material have excellent Optical property [1,2]. α amino acids the ability has molecular chirality, weak vander waals, Hydrogen bonds and zwitterionic nature of a molecule. The positively charged NH_3

amino acid Asparagine monohydrate molecule (cation) and the negatively charged COOH group of the malic acid (anion) are interconnected via a hydrogen bonds created through proton transfer in a head to tail arrangement. A Strong electron donor and acceptor groups are generated on the either side of the conjugated π -Electron. L-Asparagine Monohydrate ($C_4H_{10}O_4N_2$) admixtured with DL- Malic acid ($C_4H_6O_5$) (LAMDLM) organic single crystal has Orthorhombic structure with the space group of $P2_12_12_1$. The unit cell parameters are a = 9.821, b = 11.80, c = 5.587, V = 647.79. L-Asparagine monohydrate was observed in certain amino acid examples of L-Asparagine tartarate, L-Asparginium picrate, L-Asparagine nitrate, L-Asparagine oxalate are proved to be potential materials for Nonlinear optical applications [3-6]. In this experimental work, LAMDLM crystals was synthesis by slow evapouration method at room temperature. The physical phase and cell parameters were identified by powder X-Ray diffraction analyses. FTIR spectrum was used to identify the functional groups. UV-Vis analysis was carried towards optical properties. The present study LAMDLM single crytals and analysis its Nonlinear optical properties [7-11]. The grown crystals was subjected into various studies such as Energy dispersive X-ray analysis (EDAX), scanning electron microscopy (SEM) and Laser damage threshold are reported.

2.Experimental

2.1. Material Synthesis

LAMDLM Crystal have a tendency to polarization reversal at room temperature. In order to overcome this difficulty there have been deionized water solvents are added. In this work L-Asparagine malate is selected as pure. L-Asparagine monohydrate (Extra pure CHR, 99%) admixtured with DL-Malic acid (minimum assay, 99.0% purity) was taken in 1:1 ratio were carried out. The reaction of the synthesis is shown here as

$$C_4H_{10}N_2O_4 + C_4H_6O_5 = C_8H_{14}N_2O_8 \cdot H_2O$$

The calculated amount of L-Asparagine monohydrate admixtured DL-Malic acid were dissolved in deionized water are added at room temperature. The solution was continuous stirred well using of Magnetic stirrer for 6h the saturated solution was filtered by using whatmann filter paper and kept in a beaker. Optically transparent and well shaped crystals of 4mm x 3mm x 1mm size have been harvested after 6 months of growth. The pure solution was prepared. Calculated amount of Amino acid L-Asparagine monohydrate 5g and then organic acid of DL-Malic acid 4.5 gm of (1:1) Equimolar ratio. The calculated amount of both the materials were taken in same beaker and completely dissolved in distilled water. The saturation solution was filtered with filter papers. The growth was carried out by slow evaporation method at room temperature. After 5 to 6 months LAMDLM crystal were harvested. It is found be transparent crystal. The grown crystal is shown in the photograph fig 2.1.

Fig 2.1 As grown single crystal

2.2 Characterization techniques

The grown samples of L-Asparagine malate crystal was analysed by powder X-ray diffraction studies using an instrument Bruker D8 Advance Diffractometer were carried**.** The FTIR Studies were performed using Brucker alpha II having KBr pellet technique in the range 500 - 4500 cm^{-1}. The optical constants of LAMDLM crystals were estimated by optical absorbance spectra that were recorded in the wavelength range 190-1100 nm using Jasco V-730 Spectrophotometer. The particles size and morphology of nanoparticles were analysed by ZEEISS-SEM machine [12]. The obtained sample was investigated using a SEM/EDX scanning microscope JEOL-JSM 64000LV. The Laser damage threshold Studies

3.Results and Discussion

3.1 Powder X-Ray Diffraction (XRD) Analysis

To check the crystalline structure and phase purity of the prepared samples, powder XRD studies were carried out at room temperature. The grown samples of L-Asparagine malate crystal was analysed by powder X-ray diffraction studies using an instrument Bruker D8 Advance Diffractometer were carried**.** The data have been collected by using CuKa($\lambda = 1.5418$) radiation. Here the sample was scanned for the angular range 5°-10° of 2θ with a increament of 0.05° min. Powder XRD pattern of L-Asparagine malate crystals are shown in figure 2. The XRD pattern contains number of well defined Bragg's peaks which indicates that, samples is in crystalline phase. It is clearly seen from the figure that the peak positions of powder XRD pattern of LAMDLM matches very well with that of standard *JCPDS* data. From the single crystal belongs to orthorhombic crystallographic system with the space group $P2_12_12_1$. The unit cell paramters are a = 9.821, b = 11.80, c = 5.587, V = 647.79 and no of atoms Z = 4. The interfacial angles $\alpha = \beta = \gamma = 90°$. The lattice parameters of LAMDLM are in good agreement with the reported values. Powder X-Ray diffraction analysis carried out to confirm the physical phase of the product. Crushed powder of LAMDLM crystal was subjected to analysis in order to determine the crystal phases by XRD, From the powder X-ray diffraction pattern of grown LAMDLM, the different planes of reflection were indexed using XRD program [13,14]. The Peak position 2θ (Deg), Relative intensity, d spacing and h k l Values for L-Asparagine malate are listed in Table 1. The standard values are taken in *JCPDS* card number (30-1529) data.

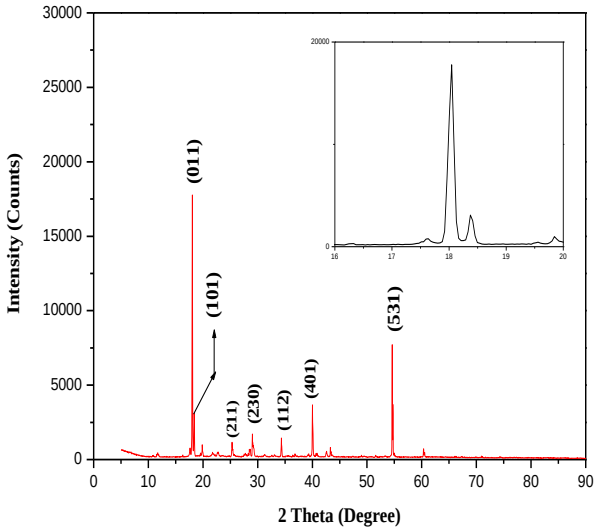

Fig 2 Powder XRD Pattern of LAMDLM Crystals

Table 1

Powder XRD Data of L-Asparagine malate

Angle (2θ degree)	Relative intensity (%)	(H K L)	d spacing
18.011	100.0	0 1 1	4.92125
18.389	20.0	1 0 1	4.82087
25.424	3.4	1 0 1	3.50062
29.130	7.0	2 3 0	3.06309
34.425	3.8	1 1 2	2.60310
39.947	10.6	4 0 1	2.25508
54.622	41.7	5 3 1	1.67888

3.2 Fourier Transform infrared spectroscopy (FTIR)

The FTIR Studies were performed using Brucker alpha II having KBr pellet technique in the range 500 - 4500 cm^{-1}. FTIR Spectra help us to determine the various functional groups present in a molecule with the absorption band exhibited in the given spectra. The recorded FTIR spectra of L-Asparagine malate crystal are shown in Fig 3 and the tentative vibrational assignments are listed in Table 2. The broad peaks observed at 3445.12 cm^{-1} in FTIR is corresponds to Characteristics of OH Stretching vibration. The Broad and sharp peaks observed at 3376.98 cm^{-1} in FTIR is corresponds to NH_3 Symmetric stretching mode. The broad peak observed at 2934.94 cm^{-1} and 3096.81 cm^{-1} in FTIR is corresponds to CH_2 Symmetric stretching mode. The small peak was observed at 2324.72 cm^{-1} in FTIR is corresponds to NH_2 stretching mode. The broad and strong peaks was observed at 2518.55 cm^{-1} and 2646.66 cm^{-1} are due to hydrogen Bonded OH group. The sharp peak observed at 1679.43 cm^{-1} in FTIR is corresponds to deformation mode of NH_2 group. The Broad and sharp peaks observed at 1631.85 cm^{-1} in FTIR is corresponds to NH_3^+ asymmetric deformation mode. A sharp peak observed at 1516.81 and 1581.77 cm^{-1} corresponds at NH_3^+ symmetric stretching mode. A sharp peak observed at 1301.52 cm^{-1} and 1423.25 corresponds to CH_2 Bending deformation. The sharp peak observed at and 1352.04 cm^{-1} corresponds to CH_2 rocking vibration. The peak observed at 1225.33 cm^{-1} corresponds to Characteristics of CH_2 rocking vibration. The sharp peak observed at 1107.90 and 1141.59 cm^{-1} corresponds to C-H in plane bending vibration. The sharp peak observed at 1068.92 cm^{-1} corresponds to CH_2 rocking out vibration. The small peak observed at 890.00 cm^{-1} corresponds to wagging mode of NH_2 group. The sharp peak observed at 803.44 cm^{-1} corresponds to C-C stretching mode. The Broad and Strong Bands peak observed at 665.30 cm^{-1} corresponds to COO^- in plane bending mode [15].

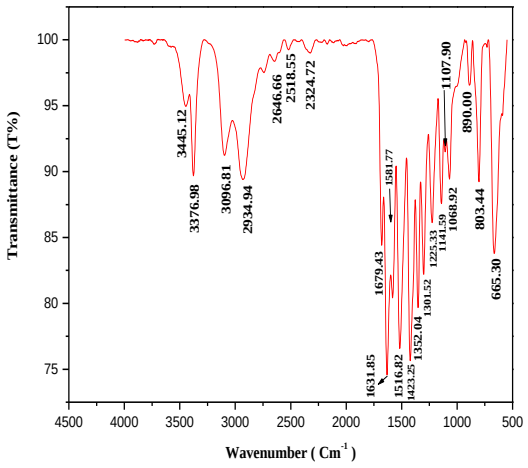

Fig 3 FTIR Spectrum of LAMDLM Crystals

Table 2

The FTIR Bands and their assignments

Wave number (cm^{-1})	**Tentative assignments**
3445.12	Characteristics of OH Stretching vibration
3376.98	NH_3 Symmetric stretching Mode
3096.81 & 2934.94	CH_2 Symmetric stretching Mode
2646.66 & 2518.55	Hydrogen Bonded OH group
2324.72	NH_2 stretching Mode
1679.43	Deformation mode of NH_2 group
1631.85	NH_3^+ asymmetric deformation mode
1581.77 & 1516.82	CH_2 Bending deformation
1352.04	CH_2 rocking vibration
1225.33	Charactersitics of CH_2 rocking vibration
1141.59 & 1107.59	C-H in plane bending vibration
1068.92	CH_2 rocking out vibration

890.00	wagging mode of NH_2 group
803.44	C-C stretching mode
665.30	COO^- in plane bending mode

3.3 UV-vis Spectroscopy

The optical constants of LAMDLM crystals were estimated by optical absorbance spectra that were recorded in the wavelength range 190-1100 nm using Jasco V-730 Spectrophotometer. The recorded UV-vis spectrum absorbance is depicted in Fig 4. The obtained transmittance spectrum for LAMDLM crystals is shown in Fig 5. The recorded UV-vis spectrum and it has good transparency of about 90% with lower cut-off wavelength 283nm [16]. The lower cut-off wavelength is due to the n- π^* transition of the carbonyl group of the carboxyl function. Good optical transparency and lower cut-off wavelength between 190 to 1100 nm are the key factors for efficient LAMDLM crystal [17]. The L-Asparagine malate crystals is active in the entire visible region, The direct band gap energy calculated from the transmission spectra by using the following relation:

$$E_g = hc/\lambda c \text{ (eV)} \quad (1)$$

Where E_g is the band gap energy, h= 6.626×10^{-34} js, C= 3×10^8 $ms^{-1,}$ and λ_c is the UV cut off wavelength, which is equal to 283nm. On substituting these values, the optical band gap energy is found to be E_g = 4.50 eV. Band gap energy plays a significant role in the determination of electrical conductivity of solids [18]. The optical properties may also be closely related to the material's atomic structure, electronic band structure and electrical properties. Knowledge of optical constants of a material such as optical band gap is quite essential to examine the materials's potential opto-electronic applications.

The optical absorption coefficient α has been calculated using the following relation:

$$\alpha = 2.303\times\text{Absorbance/t}(cm^{-1}) \quad (2)$$

Where T is the transmittance and t is the thickness of the crystal. Transfer of electrons between energy level in material scan take place in different ways.

$$(Ahv)^2 = A\,(hv-E_g) \quad (3)$$

Where 'h' is the plank's constant, 'v' frequency of vibration, 'E_g' optical band gap and 'A' a proportionality constant. The transition number(n) is 1/2 for Indirect allow transition. The value of the exponent 'n' denotes the nature of the sample transition. Here n=2 because only the direct allowed sample transition is considered in LAMDLM crystal [19,20]. The optical band gap of LAMDLM single crystal is evaluated by the linear extrapolation of the Tauc's graph plot between $(\alpha hv)^2$ and (hv) to the energy axis. The variation of $(\alpha hv)^2$ versus (hv) in the fundamental absorption region is plotted in Fig 6. In UV-vis wavelength and absorbance peaks are shown in Fig 3.6. The UV-vis wavelength and absorbance peak values (Table 3.3). The optical direct band gap of LAMDLM crystals is found to be E_g=

4.50 eV.

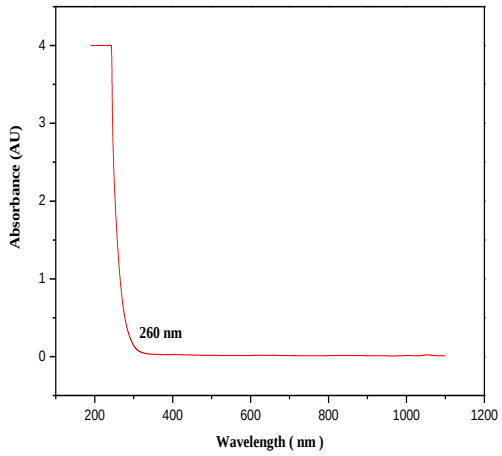

Fig 4 UV-vis absorbance of LAMDLM crystals

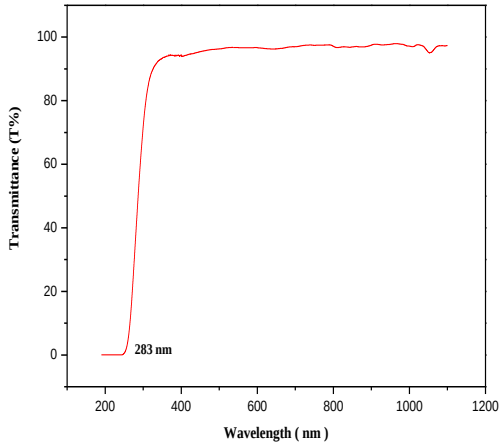

Fig 5 UV-vis Transmittance of LAMDLM crystals

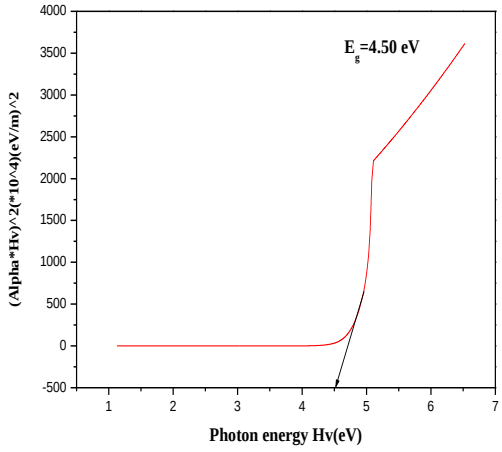

Fig 6 UV vis Energy band gap of LAMDLM crystals

3.4 Scanning Electron Microscopy (SEM)

From Fig 7 to Fig 10 shows the SEM Micrographs of particle size in LAMDLM crystals. The particles size and morphology of nanoparticles were analysed by ZEEISS-SEM machine. The dried form of silver nanoparticles were sonicated with distilled water, small droplet of silver nanoparticles were placed on glass slide and permitted to dry. The ZEEISS- SEM machine was worked at a vaccum of the order of 10-5 torr. The accelerating voltage is 10 KV. The particle size of nanoparticles can be analyzed by using image magnification software compatible with SEM. The Scanning electron microscope (SEM) analysis of particles as shown in Fig 11. Scanning Electron microscopical (SEM) and particle size analysis SEM analysis was carried out to understand the topology and the size of the particles, which showed the synthesis of higher density polydispersed particles of various sizes that ranged from 92 to 117nm and crystalline nature of the nanoparticles. Most of the nanoparticles gathered and only a little of hem were dispersed, when observed under SEM. To find out the particle size of the nanoparticles using histograms plotted on the obtained data to study the particle size distribution using Image J software and the size of the nanoparticles ranged from 92.15 to 118.70nm and the average particle size was found to be 104.63 ± 9.24nm [21]. The Histogram showing particle size distribution of particle as shown in Fig 12.

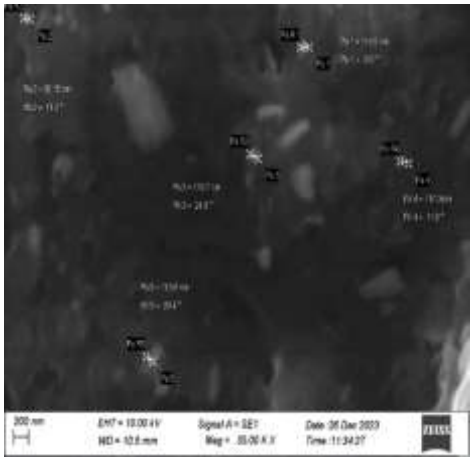

Fig 7 a). SEM micrograph

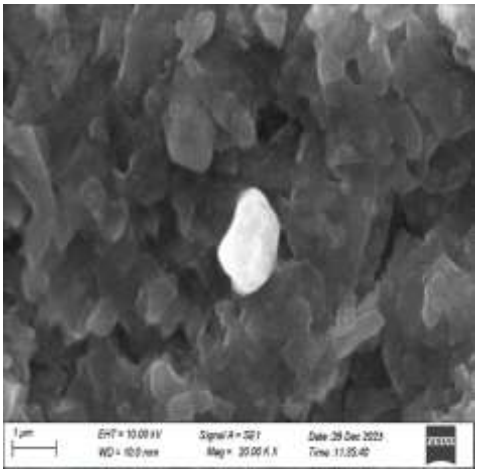

Fig 8 b) SEM micrograph

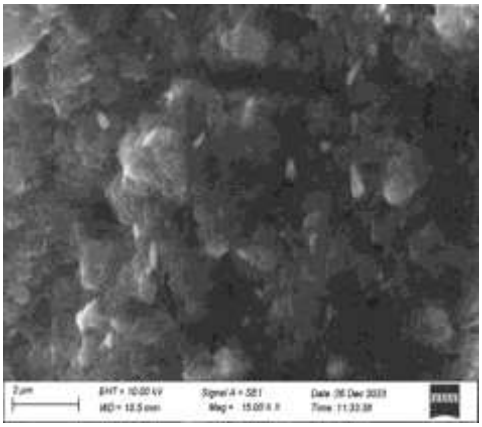

Fig 9 c) SEM micrograph

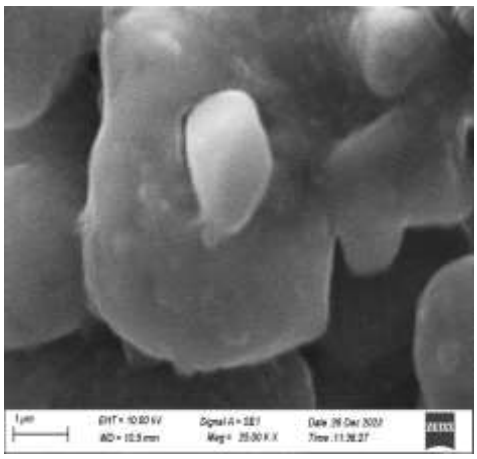

Fig 10 d) SEM micrograph

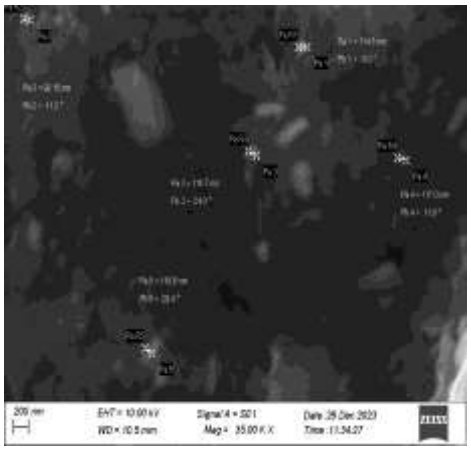

Fig 11 Scanning Electron Microscope (SEM) analysis of particles

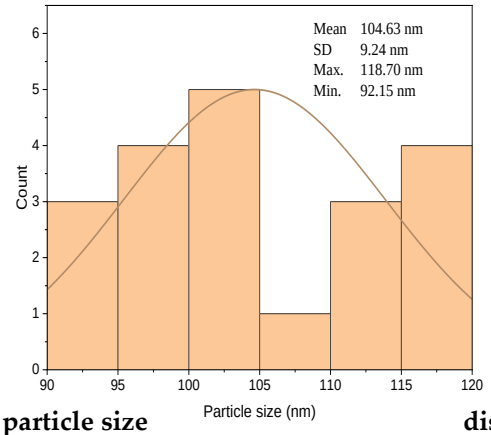

Fig 12 Histogram showing particle size distribution of particle

3.5 Energy dispersive X-ray analysis (EDAX) Analysis

EDAX Spectrum of LAMDLM shown in fig 13. The obtained sample was investigated using a SEM/EDX scanning microscope JEOL-JSM 64000LV. Energy dispersive X-ray analysis measurements were performed under standard conditions [22-24]. Energy dispersive X-ray analysis (EDAX) has become an important tool for characterizing the elements present in the crystal. The recorded EDAX spectrum shows the presence of Carbon, Nitrogen and oxygen element which may be due to incorporation of L-asparagine malate in the material of grown crystal [25-28]. The presence of C, N, O in the LAMDLM is confirmed by EDX shown in table 3.

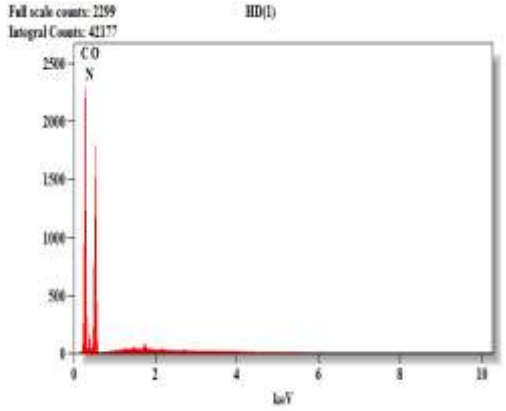

Fig 13 EDAX spectrum of L-Asparagine malate

Table 3

Quantitative results for: HD(1)

Element	Net counts	Weight%	Atom %	Atom% Error	Formula
C	12676	25.81	31.03	±0.29	C
N	1593	15.47	15.95	±1.16	N
O	10760	58.72	53.01	±0.64	O
Total		100.00	100.00		

3.6 Laser Damage Threshold

The Laser damage threshold Studies were performed using an instrument Q-switched High Energy Nd:YAG (QUANTA RAY Model: LAB-170-10). The efficiency of NLO Crystal depends not only on the linear and NLO properties, it also depends on its aptitude to with stand high power lasers. The laser damage threshold value of LAMDLM crystals has been determined using Q- switched Nd: YAG: Laser for pulse width τ = 6 ns laser pulses at a wavelength of 1064 nm. The energy of the beam was augmented from 6.9 mJ and the focal length of the Biconvex lens laser beam is 10 cm. The repetation rate is 10Hz.

The power density,

$$(P_d)=E/\tau\pi r^2 \qquad (4)$$

Where E is the input energy mJ , τ the pulse width and r the radius of the beam. The measured multi shot laser damage Threshold (LDT) value for grown LAMDLM crystal is 3.6 GW/cm^2, The LDT value of LAMDLM is comparable with high excellence NLO crystals. Superior value of LDT designated that a grown crystal contains low defect. Hence, the LAMDLM crystal can be used for NLO and related high power laser applications due to its superior laser damage threshold values [29]. . It is seen from table 4 that the laser damage threshold (LDT) value for LAMDLM crystals.

Table 4

The Laser Damage Threshold values for LAMDLM Crystals

S. No	Name of the sample	Output Energy (Milli Joule)	LDT Value (GW/cm^2)
1	L-Asparagine malate	6.9	3.6

4. Conclusion

Colourless and transparent LAMDLM crystals have been grown by solution method with slow evaporation techniques. L- Asparagine monohydrate admixtured with DL- Malic acid was successfully prepared. The grown crystal have been subjected to various studies like powder XRD, FTIR, UV-Visible spectroscopy, SEM, EDAX and Laser damage threshold (LDT) studies. In powder XRD studies confirmed that LAMDLM crystals in orthorhombic system with the space group $P2_12_12_1$. The Functional group of the LAMDLM crystals have been identified by FTIR studies. The UV-vis analysis shows that the sample is optically Transparent (90%) over a wide wavelength region. The optical absorption study revealed that the crystal has a low absorption with UV cut-off wavelength around 260nm. From UV visible analysis says that the transparency of LAMDLM crystal has a cut-off wavelength around 283nm. In UV-vis direct band gap energy E_g is 4.50 eV respectively. In LAMDLM Crystal the Multilayer plate-like pattern of growth was observed by Scanning electron microscopy. The presence of L-Asparagine malate was confirmed by EDAX analysis. Incorporation of Various C, N, O are the elements present in L-Asparagine malate in the crystal was confirmed by Energy Dispersive X-ray Analysis (EDX). Hence,

the measured multiple shot laser damage Threshold (LDT) value for grown LAMDLM crystal is 3.6 GW/cm^2.

Aknowledgements

The gratefully acknowledge to my guide Dr. K. Balasubramanian, The M.D.T Hindu college, Department of physics, pettai- 627010. I am Thankful to "SAVEETHA INSTITUE OF RESEARCH CENTRE, CRESCENT INSTITUTE OF SCIENCE AND TECHNOLOGY and HARMAN INSTITUTE OF RESEARCH CENTRE" For providing to access the DST-FIST sponsored instrumentation facilities such as XRD, FTIR, UV, LDT, EDAX and SEM etc., to our college.

References

1. S. O. Pillai, "Solid state physics", Third edition, New Age international (P) Limited, New Delhi, (1999).
2. Rani. R, Thukral K, Krishna A, Sharma G, Vijayan N, Rathi B, and Bagavannarayana G, 2014 synthesis and nucleation studies on L-leucine hydrobromide: a promising nonlinear optical material J. applied cryst. 47 1966-1974.
3. C. Kittle, "Introduction to solid state physics", Wiley Eastern ltd., New delhi, (1976).
4. WWW.wikipedia.org.
5. A. J. Dekkar "Solid state physics", Macmillan India Limited, New Delhi, (1998).
6. P. Santhana Raghavan and P. Ramasamy, "Crystal growth Processes and Methods", KRU Publucations, Kumbakonam, (2003).
7. M. J. Rosker and C. L. Tang, "Widely Tunable optical parametric oscillator using Urea', J. Opt, Soc, Am. (B), (1985), Vol. 2, pp. 691-695.
8. B. Huang, S. Genbo and H. Youping, "Growth of large size urea crystals", J.Cryst growth, (1990), Vol. 102, pp.762-764.
9. D. S. Chemla and J. Zyss, "Nonlinear optical properties of Organic molecules and crystals", Academic press, New York, (1987), Vol. 1 & 2.
10. V. Raghavan "Materials science and Engineering" Prentice Hall, New delhi, (1985).
11. K. Nakamoto, "Infrared and Raman Spectra of Inorganic and Coordination compounds, "John wiley and Sons, New York, (1978).
12. J. P. Benson and E. K. Gill "Crystal structure analysis", Oxford university Press, New York, (1966).
13. B. E. Warren, "X-Ray diffraction", Addison Wesley, California, (1969).
14. B. D. Cullity, Elements of X-Ray diffraction, Pearson Education, (1956).
15. S. Masilamani, A. Mohamed Musthafa chemical analysis, FTIR and microhardness study to find out nonlinear optical property of L-Asparagine lithium chloride: a semiorganic crystal microchemical journal 110 (2013) 749-752.
16. Nakatani, Jpn. J.Appl. phys, (1990), Vol. 29, pp. 2774.
17. N.Nakatani, Jpn. J.Appl. Phys, (1993), Vol. 32, pp. 4268.
18. G. Ravi, S. Anbukumar, P. Ramasamy, J.Crys Growth, (1993), Vol. 133, pp. 272.
19. P. J. Lock, Appl, Phys. Lett, (1971), Vol. 19 pp. 300.
20. K. Syed Suresh Babu, M. Anbucheziyan, M. Gulam Mohamed, P. A. Abdullah Mahaboob, R- Mohan, Growth, optical, Dielectric, thermal and mechanical properties of pure and Sr (2)-doped L-Asparagine monohydrate single crystals (LASP), Arch. Phys. Res, (2013), Vol: 4(2), pp. 31-39.
21. A. Hamid, A Beginners Guide to scanning electron microcopy, Spinger, (2018).

22. T.S. Shyju, S. Anandhi, R. Gopalakrishnan, Comparative studies on conventional solution and Sankaranarayanan- Ramasamy (SR) methods grown potassium sodium tartarate
23. tetrahydrate single crystals, cryst. Eng. Commun, (2012), Vol. 14, pp. 1387-1396.
24. Robert M. Silverstein, Francis X, Webster, David J.Kiemle, Spectrometric Identification of organic compounds, Seventh ed., John wiley, USA, (2005), pp. 105-106.
25. P. A. Illenkhena, Optical characterization and possible solar energy applications of improved solution grown cobalt oxide (CoO) thin films at 300K, African Phys. Rev, (2008), Vol. 2, pp. 68-77.
26. F. El-Diasty, A. Abdul waheb, optical Band gap studies on lithium aluminium silicate glasses doped with Cr^{3+} ions, J, Appl, Phys, (2006), Vol. 100, pp. 093511-1-093511-7.
27. P. V. Dhanaraj, T. Suthan, N. P. Rajesh, synthesis, crystal growth and characterization of a semiorganic material: calcium dibromide bis (glycine) tetrahydrate, curr, Appl, Phys, (2010), Vol. 10, pp. 1349-1353.
28. F. Q. Meng, M. K. Lu, Z. H, Yang, H. Zeng, Thermal and Crystallographic properties of a new NLO Material, Urea-(D) tartaric acid single crystal, Mater. Lett, (1998), Vol. 33, pp. 265-268.
29. S. Masilamani, K. Tamilarasan, Synthesis, growth and characterization of L-Asparagine cadmium bromide: a novel semi organic nonlinear optical single crystal, Optik, (2013), Vol. 124, pp. 4303-4306.
30. S. K. Kurtz and T. Perry, A powder technique for the evaluation of Nonlinear optical materials, J.Applied physics 39(8) (1968) 3798-3813.
31. N. Rajasekar, Ph.D. project, The M.D.T Hindu college, (2024).